Joint Estimation of Channel, Range, and Doppler for FMCW Radar with Sparse Bayesian Learning

Mehdi Ashury*†, Fangqing Xiao‡, José Rodríguez-Piñeiro§, Dirk Slock‡,
Peter Gerstoft¶, Christoph F. Mecklenbräuker†, Dominik Lungenschmied*
*Infineon Technologies, Linz, Austria
†Institute of Telecommunications, TU Wien, Vienna, Austria
‡EURECOM, Sophia-Antipolis, France
§College of Electronics and Information Engineering, Tongji University, Shanghai, China
¶NoiseLab, UC San Diego, La Jolla, CA

***Abstract*—The adoption of Advanced Driver Assistance Systems (ADAS) and autonomous driving systems poses great challenges for vehicular communication and sensing architectures. The joint design of vehicular communication and sensing systems brings benefits both in performance, size, cost, and power consumption, and it enables cooperative perception, in which the local information from all vehicles is fused. We propose using joint estimation of channel, range, and Doppler frequency for Frequency Modulated Continuous Wave (FMCW) radar. Based on Sparse Bayesian Learning (SBL), this enables the use of prior knowledge (as local estimates from neighboring vehicles) in the data processing. This provides more reliable and accurate sensing than traditional radars, which only rely on the detection of LOS objects for a single vehicle. Besides, SBL increases the channel estimation accuracy, which constitutes a basis for the optimization of the transceivers/sensing nodes and reduces the probability of false alarm. Our represents an efficient framework for cooperative sensing in ADAS applications and contributes to the convergence of communication and sensing applications for connected vehicles.**

***Index Terms*—Wireless Channel, Automotive sensors, FMCW radar, Sparse Bayesian Learning**

I. Introduction

With the recent rise of Advanced Driver Assistance Systems (ADAS) and the incipient adoption of autonomous driving solutions, the requirements for both communications and sensing solutions for vehicles have significantly increased. On the one hand, efficient and timely communication among vehicles and infrastructure elements, or between neighboring vehicles, is essential to adapt to time-variant scenarios of road environments, ensuring safe and efficient transportation. Cooperative Awareness Messages (CAM) can be exchanged among adjacent road users via Cooperative Vehicle-to-Anything (C-V2X) connectivity [1]. At the same time, sensing the environment is critical for collision avoidance and to match the actual environment to pre-loaded mapping information in autonomous driving.

Neither vehicular communications nor radar applications for vehicles are novel, nevertheless, their use in real-time autonomous driving applications presents several challenges. On the one hand, due to the constraints of mass-production vehicles, onboard radar systems are limited in size, computational power, and cost. At the same time, advanced applications require the resolution of the sensing environment to be increased as much as possible, to deal with several close-range scatterers in dense urban environments. On the other hand, a set of different communication links may be required, such as [2] vehicle-to-vehicle transmissions (to share attributes with neighboring vehicles), vehicle-to-infrastructure (to facilitate intelligent road management), vehicle-to-pedestrian (for warning or alarming purposes) and vehicle-to-network (for general purpose data transmission). These communications may have very different data traffic patterns and different requirements on throughput, latency, and reliability.

Due to all this, the coexistence between radar and communication systems using overlapping frequency bands has experienced a surge of research interest in recent years [3]. What is more, with the upcoming of Integrated Communication and Sensing (ISAC), the joint design of communication and sensing strategies can bring benefits not only in performance but also gains in size, cost, and power consumption optimization [2]. At the same time, connectivity between neighboring vehicles enables cooperative sensing, in which the local sensing information from all the vehicles is fused [4].

Since for both communication and sensing, accurate channel estimation is fundamental for the optimization of the transceivers/sensing nodes [5] and the discrimination of false targets [6], we propose the joint estimation of channel, range and Doppler frequency for Frequency Modulated Continuous Wave (FMCW) radar. Based on Sparse Bayesian Learning (SBL) [7], this enables using prior knowledge (e.g., local estimates from neighboring vehicles) in the data processing. This enables a richer sensing accuracy than that solely based on the detection of objects in the LOS to a single vehicle, as provided by traditional radar systems.

In [8], the target scene is estimated based on a sparse representation in the range-Doppler domain and a robust Bayesian algorithm mitigates the grid mismatch in both the range and Doppler dimensions.

A probabilistic model is derived in [9] where a hierarchical sparsity-promoting prior is imposed over the scatter coefficients. This leads to a sparse variational Bayesian approach with modified automatic relevance determination.

Our contributions can be summarized as follows: (1) Application of SBL to the beat frequency signal of a 76 GHz FMCW radar for the detection of multiple radar targets, and estimation of their ranges and Doppler shifts; (2) By incorporating priors for range and Doppler into the SBL framework, the detection of weak radar targets is enhanced (3) CAM messages shared among adjacent road users provide the prior information for SBL. Our work represents an efficient framework for cooperative sensing in ADAS applications and contributes to the convergence of communication and sensing applications for connected vehicles.

The rest of the paper is organized as follows: Section II introduces the basic concepts and signal model used. Section III introduces the concept of SBL for radar. Section V introduces the architecture used for the empirical evaluations, whereas Section VI analyzes the obtained results. Finally, Section VII introduces the concluding remarks of the work.

II. Radar beat frequency signal model

We consider a propagation channel with time-variant channel impulse response $h(t,\tau)$ between the transmitter and receiver antennas [10],

$$h(t,\tau)=\sum_{p=1}^{P}\gamma_p \mathrm{e}^{j\omega_{\mathrm{D}p}t}\delta(\tau-\tau_p). \quad (1)$$

Here, the channel impulse response contains P radar targets, each of which is parameterized by its propagation delay τ_p, Doppler shift $\omega_{\mathrm{D}p}$, and complex-valued radar target coefficient γ_p. The transmitted signal $x(t)$ is modeled by L repetitions of the known Linearly Frequency Modulated (LFM) waveform $s(t)$,

$$x(t)=\sum_{\ell=1}^{L}s(t-(\ell-1)T_s), \quad (2)$$

where T_s is the repetition period. The received signal is a linearly filtered version of $x(t)$ corrupted by additive noise $w(t)$. The equivalent complex baseband signal is

$$r(t)=\int_{-\infty}^{\infty}x(\tau)h(t,t-\tau)d\tau+w(t). \quad (3)$$

Inserting the model (1) into (3) gives

$$r(t)=\sum_{p=1}^{P}\gamma_p \mathrm{e}^{\mathrm{j}\omega_{\mathrm{D}p}t}x(t-\tau_p)+w(t), \quad (4)$$

Next, we use (2), giving

$$r(t)=\sum_{\ell=1}^{L}\sum_{p=1}^{P}\gamma_p \mathrm{e}^{\mathrm{j}\omega_{\mathrm{D}p}t}s(t-(\ell-1)T_s-\tau_p)+w(t). \quad (5)$$

The output from the radar module is the discrete-time radar beat frequency signal, namely $y[t]$, obtained from

$$y(t)=\int_{-\infty}^{\infty}r(\tau)x^*(t+\tau)\,\mathrm{d}\tau, \quad (6)$$

In practice, Low Pass Filtering (LPF) and subsequent A/D conversion (ADC) are used to obtain $y[t]$. The relevant parameters regarding the ADC and the LPF are listed in Table I. Due to the excellent cross-correlation properties of the LFM waveform and the frontend analog signal processing, the radar beat frequency signal $y[t]$ contains sinusoidal signal components, one for each radar target. The frequency of an individual signal component is proportional to the radar target's range.

TABLE I
Common measurement parameter setting.

Name	Symbol	Value
Chirp start frequency	f_0	76 GHz
FMCW bandwidth	BW	700 MHz
Number of chirps	L	256
Chirp duration	T_{chirp}	50 μs
Samples per chirp snapshot	N	625
Period of a chirp	T_s	63.92μs
ADC resolution		14 bit
ADC sample frequency	f_s	50 MHz
ADC decimation factor	D	4
Low pass filter	$\mathrm{BW}_{\mathrm{LPF}}$	17.3 MHz
Transmit power	P_{tx}	14 dBm
Number of radar TX antenna		1
Number of radar RX antenna		1
TX and RX antenna gain		24 dBi

The data matrix is $\boldsymbol{Y}=[\boldsymbol{y}_1,\ldots,\boldsymbol{y}_L]\in\mathbb{C}^{N\times L}$ with the ℓth column vector $\boldsymbol{y}_\ell$ being the ℓth chirp snapshot,

$$\boldsymbol{y}_\ell=[y_{1\ell},\ldots,y_{N\ell}]^T\in\mathbb{C}^N. \quad (7)$$

and elements

$$y_{n\ell}=y[(n-1)\Delta\tau+(\ell-1)T_s], \quad (8)$$

where $n=1,\ldots,N$ is the range sample index, $\ell=1,\ldots,L$ is the chirp index, and $N\Delta\tau=T_{\text{chirp}}/D$. Further, we introduce the unknown complex-valued radar target vector $\boldsymbol{c}_\ell=[c_{1\ell},\ldots,c_{M\ell}]^\mathsf{T}\in\mathbb{C}^M$ for the ℓth chirp, which is assumed P-sparse, with $P\ll M$. Similarly, we define the additive noise vector $\boldsymbol{w}_\ell=[w_{1\ell},\ldots,w_{N\ell}]^\mathsf{T}\in\mathbb{C}^N$. Finally, we formulate the mapping from the radar target vector elements to the radar beat frequency signal as a sparse regression model for all chirps ($\ell=1,\ldots,L$),

$$\boldsymbol{Y}=\boldsymbol{A}\boldsymbol{C}+\boldsymbol{W}, \quad (9)$$

where $\boldsymbol{A}\in\mathbb{C}^{N\times M}$ is called the dictionary, with elements

$$A_{nm}=\mathrm{e}^{\mathrm{j}2\pi(n-1)\nu_m\Delta\tau}. \quad (10)$$

The beat frequency ν_m is associated with the target range

$$\nu_m=\frac{1}{\Delta\tau}\left(\frac{m-1}{M-1}-\frac{1}{2}\right),\ \text{for } m=1,\ldots,M. \quad (11)$$

The mth column $\boldsymbol{a}_m$ of the dictionary $\boldsymbol{A}$ models the sinusoidal beat signal component by the Vandermonde vector

$$\boldsymbol{a}_m=[1,\,\alpha_m,\,\alpha_m^2,\ldots,\alpha_m^{N-1}]^T,\quad \text{where } \alpha_m=\mathrm{e}^{\mathrm{j}2\pi\nu_m T_s} \quad (12)$$

The matrix of unknowns is $\boldsymbol{C} = [\boldsymbol{c}_1, \ldots, \boldsymbol{c}_L]$ and $\boldsymbol{W}$ is zero-mean iid noise. In the following, we estimate the unknown normalized frequencies corresponding to P radar targets by SBL [11].

III. SBL for Radar Target Coefficients and Range Estimation

We apply SBL to a single measurement vector $\boldsymbol{y}_\ell$. SBL is derived under a joint complex multivariate Gaussian assumption on $\boldsymbol{c}_\ell$ and $\boldsymbol{w}_\ell$ for each snapshot ℓ, cf. [11, Table I]. SBL provides radar target coefficient estimates based on the rank-1 sample covariance matrix

$$\boldsymbol{S}_\ell = \boldsymbol{y}_\ell \boldsymbol{y}_\ell^{\mathrm{H}}, \tag{13}$$

where $(\cdot)^{\mathrm{H}}$ denotes Hermitian transposition. The sample covariance matrix is a sufficient statistic under the joint Gaussian assumption.

For applying robust and sparse M-estimation of range and Doppler shift for individual radar targets, we assume that the data distribution of the discrete-time radar beat frequency signal vector $\boldsymbol{y}_\ell$ for the ℓth snapshot follows a Complex Elliptically Symmetric (CES) distribution with noise variance σ^2 [12], [13]. Further, the prior distribution of the radar target coefficient vector $\boldsymbol{c}_\ell$ is assumed to be zero-mean complex Gaussian with diagonal covariance matrix $\boldsymbol{\Gamma}_\ell$. Based on Bayes' rule, we estimate the posterior probability density function for the unknown radar target coefficients $\boldsymbol{c}_\ell$. Finally, the noise $\boldsymbol{w}_\ell \in \mathbb{C}^N$ is assumed independent identically distributed (iid) across samples, zero-mean, with finite variance σ^2.

If $P \geq 1$ radar targets are present, then $\boldsymbol{c}_\ell$ is P-sparse. The model (9) is underdetermined and $P < N \ll M$. The covariance matrix of $\boldsymbol{y}_\ell$ takes the form

$$\boldsymbol{\Sigma}_\ell = \boldsymbol{A}\boldsymbol{\Gamma}_\ell \boldsymbol{A}^H + \sigma^2 \boldsymbol{I}_N, \tag{14}$$

$$\boldsymbol{\Gamma}_\ell = \mathrm{diag}(\boldsymbol{g}_\ell), \tag{15}$$

where $\boldsymbol{g}_\ell = [g_{1\ell} \ldots g_{M\ell}]^T$ is the P-sparse vector of unknown radar target magnitudes which is to be estimated by the robust SBL algorithm [13]. The active set $\mathcal{M}$ is defined as

$$\mathcal{M} = \{m \in \{1, \ldots, M\} | g_{m\ell} \neq 0\}. \tag{16}$$

If $m \in \mathcal{M}$ then the mth range bin is active in the ℓth chirp snapshot and the corresponding radar target is estimated to be at a range proportional to the beat frequency ν_m.

IV. SBL for Doppler estimation

Let $\boldsymbol{A}_\mathcal{M} \in \mathbb{C}^{N \times P}$ contain the P "active" Vandermonde columns from $\boldsymbol{A}$. For Doppler estimation, we first transform the data matrix $\boldsymbol{Y}$ into the domain of active delay bins,

$$\boldsymbol{Z}_\mathcal{M} = \boldsymbol{A}_\mathcal{M}^H \boldsymbol{Y} \in \mathbb{C}^{P \times L}, \tag{17}$$

which can be computed by a fast Fourier transform. We define

$$\boldsymbol{Z}_\mathcal{M}^T = [\boldsymbol{z}_1, \ldots, \boldsymbol{z}_P] \in \mathbb{C}^{L \times P} \tag{18}$$

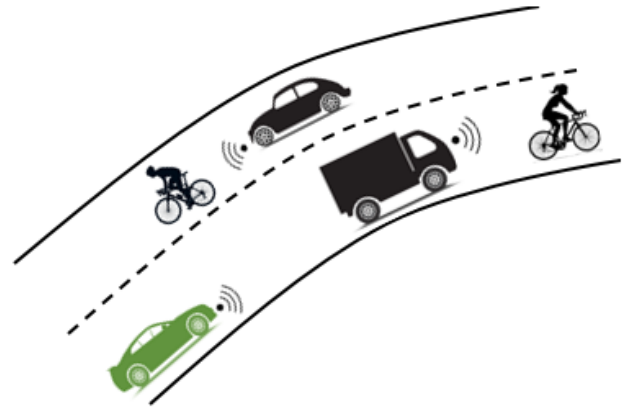

Fig. 1. Traffic scenario with NLOS between the green car and a bicycle.

and apply the SBL algorithm to each transformed data vector

$$\boldsymbol{z}_p = \boldsymbol{Y}^T \boldsymbol{A}_\mathcal{M}^* \boldsymbol{e}_p \in \mathbb{C}^{L \times 1}, \tag{19}$$

individually, where $\boldsymbol{e}_p \in \mathbb{C}^{L \times 1}$ is the pth standard unit basis vector $(p = 1, \ldots, P)$. For Doppler estimation, we use the dictionary $\boldsymbol{B} \in \mathbb{C}^{L \times Q}$ of Vandermonde vectors for Doppler estimation with column vector

$$\boldsymbol{b}_q = [1, \beta_q, \beta_q^2, \ldots, \beta_q^{L-1}]^T, \quad \text{where } \beta_q = \mathrm{e}^{\mathrm{j}\Omega_q} \tag{20}$$

and $\Omega_q = 2\pi(q-1)/Q$.

V. Considered Architecture

The architecture consists of several vehicles each with one FMCW automotive radar sensor in different road traffic scenarios. The automotive radar sensors are operating at the 77 GHz band. The communication of the radar data among the vehicles can be done with a 5G cellular network. The NLOS scenarios are common in road traffic and are a limitation and a challenge for radar sensor applications. Our proposed system can make radar sensors applicable for non-LOS scenarios. Further, automotive radars operate in a dense environment, increasing the probability of radar-to-radar mutual interference and other clutter appearances. Applying the SBL algorithm increases the detection probability and robustness compared to conventional FFT processing.

A. *Traffic Scenario*

The traffic scenario in this paper is depicted in Fig. 1, all motorized vehicles are equipped with a front radar. The green vehicle, called the "main vehicle", detects 3 targets in LOS. The bicycle in front of the truck is in NLOS to the main vehicle and cannot be directly detected by its front radar. This will lead to a dangerous situation during an overtaking scenario.

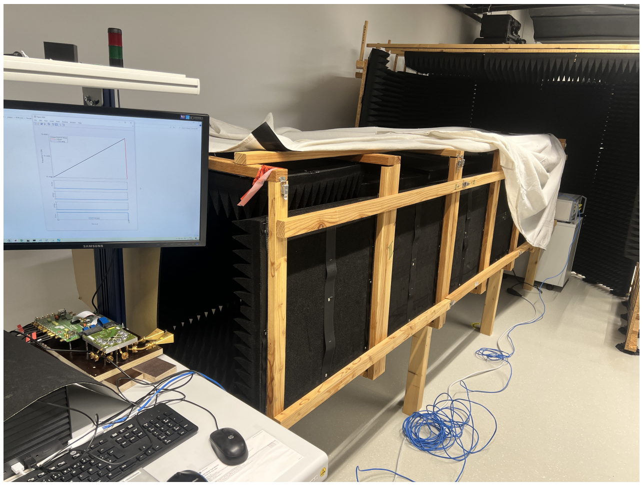

Fig. 2. Radar measurement setup: FMCW radar module, RF transmission tunnel, and RTS.

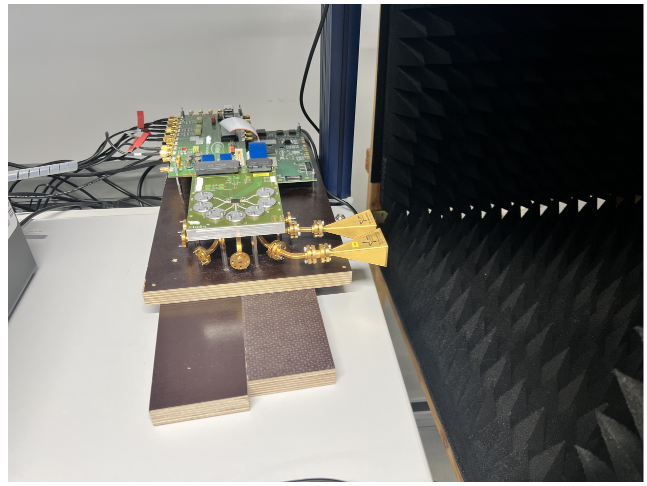

Fig. 3. Radar Measurement setup: FMCW radar module FE.

B. Data Model

The radar output signal $y(t)$, as stored in the 2D matrix $\boldsymbol{Y}$, is the discrete-time radar beat frequency signal which is obtained by analog correlation with the transmit waveform. Subsequently, there LPF and ADC are applied. The rows in the matrix $\boldsymbol{Y}$ contain the range samples and the columns contain the Doppler frequency samples. The number of columns equals the number of the transmitted chirps. We assume that a Fifth-Generation (5G) cellular network is used for communication among vehicles on the road. Each vehicle with radar sensor constantly provides the beat frequency signal $y[t]$ described in Eq. (6) of its measurement and the dictionary $\boldsymbol{A} \in \mathbb{C}^{N \times M}$ to the neighboring vehicles. Range dictionary size $M = 2500$ and Doppler dictionary size $Q = 2560$ were chosen. We also assume that the receiving vehicle radar data in LOS has accurate range, Doppler, and angle to neighboring vehicles.

VI. Experimental Data

As described in [4], the FFT-based OS-CFAR detector can estimate range and Doppler shift of the targets. Angle estimation is not feasible because the experimental setup lacks multiple RX antennas. Figure 4shows the range estimation of 3 targets based on classical OS-CFAR processing in comparison to the SBL algorithm. Figure 5 shows the corresponding estimated Doppler shifts for each of the three radar targets from which their relative velocities are inferred.

VII. Conclusion

We applied the SBL algorithm for the joint estimation of channel, range, and Doppler frequency in the field of FMCW radar. In particular, we applied SBL algorithm to the beat frequency signal of an automotive FMCW radar for range and Doppler estimation of multiple radar targets. We discussed the limitation of FFT-based CFAR detection in range resolution and the general radar limitation in NLOS

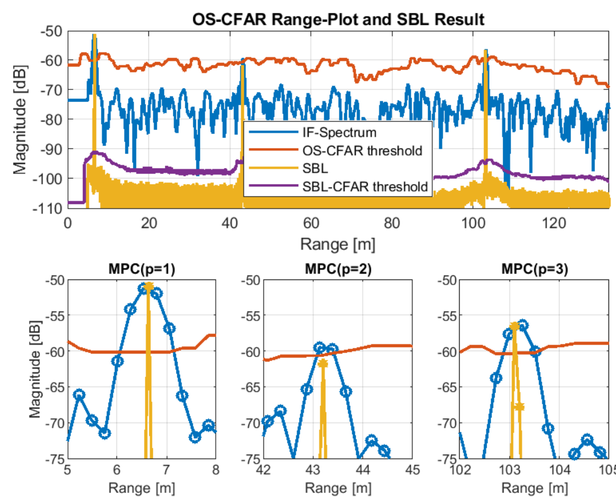

Fig. 4. Range estimates from experimental beat-frequency data for three radar targets. Top FFT-based power spectral density estimate (blue), CFAR-threshold (red), and SBL-based processing (yellow). The bottom plots zoom in on the three radar targets.

scenarios. We have proved by measurement results, that the SBL provides a higher SNR around the target peaks in the beat frequency signal. This makes the detection more reliable and decreases the probability of false alarm in a dense sensor environment with clutter and radar-to-radar interference. Our work lays the foundation for efficient cooperative sensing in ADAS applications.

References

[1] European Standard, "Intelligent Transport Systems (ITS); Vehicular Communications; Basic Set of Applications; Part 2: Specification of Cooperative Awareness Basic Service," ETSI EN 302 637-2.

[2] D. Ma, N. Shlezinger, T. Huang, Y. Liu, and Y. C. Eldar, "Joint radar-communication strategies for autonomous vehicles: Combining two key

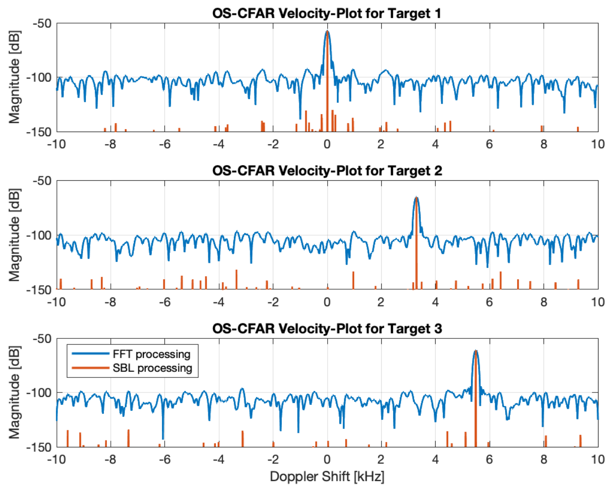

Fig. 5. Doppler shift estimation from experimental data for the same three radar targets as in Fig. 4. FFT-based power spectral density estimate (blue) and SBL-based processing (red).

automotive technologies," *IEEE Signal Processing Magazine*, vol. 37, no. 4, pp. 85–97, 2020.

[3] L. Zheng, M. Lops, Y. C. Eldar, and X. Wang, "Radar and communication coexistence: An overview: A review of recent methods," *IEEE Signal Processing Magazine*, vol. 36, no. 5, pp. 85–99, 2019.

[4] M. Ashury, P. Gerstoft, C. F. Mecklenbräuker, and D. Lungenschmied, "Channel estimation for FMCW radar with sparse bayesian learning," in *2023 IEEE Conference on Antenna Measurements and Applications (CAMA)*, 2023, pp. 266–270.

[5] M. Ashury, C. Eliasch, T. Blazek, and C. F. Mecklenbräuker, "Accuracy requirements for cooperative radar with sensor fusion," in *2020 14th European Conference on Antennas and Propagation (EuCAP)*, 2020, pp. 1–5.

[6] P. Zhu, X. Yin, J. Rodríguez-Piñeiro, Z. Chen, P. Wang, and G. Li, "Measurement-based wideband space-time channel models for 77GHz automotive radar in underground parking lots," *IEEE Transactions on Intelligent Transportation Systems*, vol. 23, no. 10, pp. 19 105–19 120, March 2022, online access: http://dx.doi.org/10.1109/TITS.2022.3157849.

[7] M. E. Tipping, "Sparse Bayesian learning and the relevance vector machine," *J. Machine Learning Research*, vol. 1, pp. 211–244, 2001.

[8] S. Bidon, M. Lasserre, O. Besson, and F. L. Chevalier, "Bayesian sparse estimation of targets with range-Doppler grid mismatch," in *IEEE Radar Conference (RadarCon)*, Arlington, VA, USA, 2015, pp. 0298–0303. [Online]. Available: https://doi.org/10.1109/RADAR.2015.7131013

[9] F. Shen, X. Chen, Y. Liu, G. Zhao, and X. Li, "Range-Doppler spectrum estimation via sparse variational Bayesian approach," *International journal of remote sensing*, vol. 40, no. 2, pp. 794–809, 2019. [Online]. Available: https://doi.org/10.1080/01431161.2018.1519279

[10] H. Groll, P. Gerstoft, M. Hofer, J. Blumenstein, T. Zemen, and C. Mecklenbräuker, "Scatterer identification by atomic norm minimization in vehicular mm-wave propagation channels," *IEEE Access*, vol. 10, pp. 102 334–102 354, 2022. [Online]. Available: https://doi.org/10.1109/ACCESS.2022.3205616

[11] P. Gerstoft, C. Mecklenbräuker, A. Xenaki, and S. Nannuru, "Multi-snapshot sparse Bayesian learning for DOA," *IEEE Signal Process. Lett.*, vol. 23, no. 10, pp. 1469–1473, 2016.

[12] C. F. Mecklenbräuker, P. Gerstoft, E. Ollila, and Y. Park, "Robust and sparse M-estimation of DOA," *Signal Processing*, vol. 220, 2024. [Online]. Available: https://doi.org/10.1016/j.sigpro.2024.109461

[13] Y. Park, E. Ollila, P. Gerstoft, and C. Mecklenbräuker, "RobustSBL Repository," in *GitHub*. https://github.com/NoiseLabUCSD/RobustSBL, 2022.